

Twist-Stabilized, Coiled Carbon Nanotube Yarns with Enhanced Capacitance

Wonkyeong Son,[▽] Sungwoo Chun,[▽] Jae Myeong Lee, Gichan Jeon, Hyeon Jun Sim, Hyeon Woo Kim, Sung Beom Cho, Dongyun Lee, Junyoung Park, Joonhyeon Jeon, Dongseok Suh,* and Changsoon Choi*



Cite This: *ACS Nano* 2022, 16, 2661–2671



Read Online

ACCESS |

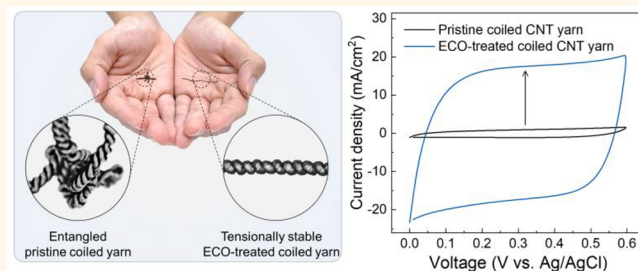
Metrics & More

Article Recommendations

Supporting Information

ABSTRACT: Coil-structured carbon nanotube (CNT) yarns have recently attracted considerable attention. However, structural instability due to heavy twist insertion, and inherent hydrophobicity restrict its wider application. We report a twist-stable and hydrophilic coiled CNT yarn produced by the facile electrochemical oxidation (ECO) method. The ECO-treated coiled CNT yarn is prepared by applying low potentiostatic voltages (3.0–4.5 V vs Ag/AgCl) between the coiled CNT yarn and a counter electrode immersed in an electrolyte for 10–30 s. Notably, a large volume expansion of the coiled CNT yarns prepared by electrochemical charge injection produces morphological changes, such as surface microbuckling and large reductions in the yarn bias angle and diameter, resulting in the twist-stability of the dried ECO-treated coiled CNT yarns with increased yarn density. The resulting yarns are well functionalized with oxygen-containing groups; they exhibit extrinsic hydrophilicity and significantly improved capacitance (approximately 17-fold). We quantitatively explain the origin of the capacitance improvement using theoretical simulations and experimental observations. Stretchable supercapacitors fabricated with the ECO-treated coiled CNT yarns show high capacitance (12.48 mF/cm and 172.93 mF/cm², respectively) and great stretchability (80%). Moreover, the ECO-treated coiled CNT yarns are strong enough to be woven into a mask as wearable supercapacitors.

KEYWORDS: *twist-stability, coiled carbon nanotube yarn, supercapacitor, hydrophilicity, electrochemical oxidation*



Multifunctional carbon nanotube (CNT) yarns or fibers have recently stimulated enormous research interest due to their attractive properties, such as high strength-to-weight ratio, unlimited yarn length, and high electrical conductivity.^{1–4} Generally, CNT yarns are fabricated by continuous drawing and spinning of bundles of nanotubes from a vertically aligned forest or a gas-carried aerogel.^{1–3,5,6} A tight twist of individual CNTs can induce close contact and strong interaction between nanotube filaments (e.g., van der Waals force), resulting in highly compacted one-dimensional (1-D) yarn structures. A straight CNT yarn can be transformed into a regular coil shape by overtwisting owing to its high mechanical strength, toughness, and outstanding flexibility.^{7,8} Coiled CNT yarns exhibit significantly improved tensile strain and stretchability. Such advantages that are superior to noncoiled yarns have promoted many exciting applications, including high-performance artificial muscles,^{9–19} stretchable supercapacitor^{20–25} or battery electrodes,^{26,27} and a variety of coiled yarn-based sensors.^{8,28–33}

Nevertheless, most coil-structured CNT yarns still suffer from two constraints that seriously restrict their practical use in

widespread applications. The first constraint is the structural instability of the yarn derived from excessively applied torsional stress. Twisted and coiled neat yarns tend to untwist or snarl when they are torsionally or tensionally unconstrained, respectively.^{8,12,29,31} This instability can be ascribed to the interspace that remains between adjacent nanotubes in the yarns due to the limited twisting angle, which is hard to control.³⁴ The void space among nanotube bundles in the yarns usually induces small yarn density and poor mechanical properties, leading to the reduction of the performance of the yarns.^{35,36} It has previously been reported that tension annealing the coiled CNT yarn in an air atmosphere can help to prevent unwanted untwisting by inducing the strong

Received: October 26, 2021

Accepted: January 20, 2022

Published: January 24, 2022



interfacial connection among CNTs; however, it requires extreme conditions (~ 2000 °C of heat treatment under 5.5×10^{-6} bar).¹² Alternatively, self-plied yarn structures that are torque-balanced by folding a coiled yarn onto itself at the yarn midpoint have been proposed.^{15,19,37} Notably, relative rotation of yarn ends can be prohibited without the help of any external tethering. However, the fundamental problem is short-circuiting of the two yarn electrodes and small element size challenges, which are essential properties for wearable electronics. Therefore, relaxing internal torsional stress with increased yarn density is of great importance for both twist retention and structural stabilization. The second constraint, especially when they are used in aqueous environments, is their intrinsic hydrophobicity originating from inert graphitic carbon–carbon bonding.³⁸ Several strategies have been reported to induce extrinsic hydrophilicity in CNT yarns. Chemical oxidation^{39,40} and acid treatment⁴¹ have been widely used for the functionalization of hydrophilic groups onto the CNT surface. Although the functionalized CNTs can exhibit improved strength or toughness after postpolymer infiltration, the harsh conditions in the acid bath generally reduce the inherent mechanical properties of the CNTs due to sp^3 defects with the destruction of the $\pi-\pi$ conjugation structure.^{42–44} Plasma treatment and organic sputtering⁴⁵ has been substantially studied to overcome this issue due to their feasibility, nonpolluting nature, and shorter treatment time. Specifically, it has been demonstrated that plasma-treated CNT yarns^{46–52} can be used for applications requiring wettability, such as electrical energy harvesting from water,⁴⁶ water/moisture-driven torsional actuators,⁴⁷ and aqueous electrolyte-based supercapacitors.^{48,49} Unfortunately, this conventional manner requires large complex facilities for gas-flow control and a vacuum environment (0.1 mbar) despite the wide versatility; furthermore, much electricity is consumed to discharge inert gas into the plasma state (e.g., 100–300 W).^{46–52} Electrochemical oxidation (ECO), as a simple and cost/energy effective oxidation method, is more suitable, and it is optimized to bestow extrinsic hydrophilicity in low dimensional and tiny electrodes, such as CNT yarns with diameters on a scale of a few micrometers.

We present a versatile method to fabricate twist stable and hydrophilic coiled CNT yarn *via* a facile ECO treatment. The resulting coiled CNT yarns were mainly functionalized with hydroxyl (C–OH) and epoxy (C–O–C) groups. Furthermore, the degree of functionalization was largely adjustable by controlling the main parameters, such as applied voltage and oxidation time. The wettability of the ECO-treated coiled CNT yarns was confirmed through both simulations and experiments, indicating that the calculated degree of charge transfer from a single water molecule to CNT increases and the water contact angle decreases after ECO treatment. More importantly, the coiled CNT yarns went through extraordinary volume expansion due to a massive double-layer charge injection during oxidation *via* the electrochemical method. The yarn shrinkage during drying from this largely expanded state increased the bulk density of the yarns and relaxed the initially introduced torsional stress with surface buckling. As a result, ECO-treated coiled CNT yarns could provide structural stability similar to heavily twisted but noncoiled yarns, which enabled a self-supporting structure without the need for an additional substrate or tethering that may otherwise untwist or become entangled.

Furthermore, we also investigate the utilization of twist-stabilized, coiled CNT yarns as supercapacitors that exploit electrical double-layer capacitance (EDLC) to provide the combination of high energy density and fast charge/discharge.²⁴ The challenge in CNT yarn-based wearable supercapacitors is to produce supercapacitors that are capable of having high capacitance at the same time as reversible deformability over large strain ranges.^{20,22,23,25} High capacitance has been achieved by incorporating pseudocapacitive materials (e.g., transition metal oxides or conducting polymers) into the CNT yarns.^{53–57} However, their incorporation may degrade the inherent mechanical properties of the host yarns with increasing loading fraction because they are more brittle or weaker than the CNTs, which inevitably leads to low strength and deformability.²⁴ Therefore, if one can impart high charge storage capacity to these CNT yarns while maintaining their mechanical properties or deformability, it may be possible to fabricate practical power sources for wearable devices. In this perspective, the proposed ECO-treated coiled CNT yarns can exhibit their maximized capacitance while avoiding the use of brittle pseudocapacitive materials by enhancing the wettability and increasing the quantum capacitance, which balances these competing requirements without significantly compromising the mechanical properties. We further demonstrate that the CNT yarn-coiling and subsequent ECO treatment offer an advanced strategy for achieving high specific linear and areal capacitance values ($C_L = 12.48 \text{ mF cm}^{-1}$ and $C_A = 172.93 \text{ mF cm}^{-2}$, respectively) and stretchability ($\epsilon = 80\%$) with stable electrical properties.

RESULTS AND DISCUSSION

Induction of Extrinsic Hydrophilicity in the Coiled CNT Yarns *via* ECO Treatment. The pristine coiled CNT yarns were fabricated by inserting a heavy twist (5500 turns m^{-1}) into CNT spun yarns (Supporting Information, Figure S1), which were drawn from carbon multiwalled nanotubes (MWNTs) forests (see Experimental Section for further details).¹ A three-electrode system consisting of coiled CNT yarns (the working electrode), Ag/AgCl (the reference electrode), and Pt mesh (the counter electrode) immersed in 0.1 M Na_2SO_4 electrolyte (Figure 1a and Figure S2). A potentiostatic voltage was applied to the working electrode (coiled CNT yarns), which introduced oxygen-containing functional groups into the sp^2 network of the surface of the coiled CNT yarn during the treatment (see inset in Figure 1a), thereby assigning local-polarization properties. Interestingly, charge injection-induced volume expansion and diameter reduction of the coiled CNT yarns were observed during the ECO treatment and drying, respectively (Figure 1b). The increased internal pressure due to the massive electrical double-layer charge injection during ECO treatment of the coiled CNT yarns possibly caused this unusual large volume expansion.

Charge transfer interactions between water and the CNT yarns before and after the ECO treatment were calculated and compared using the density functional theory (DFT). On the basis of the assumption that the CNT yarn surface is sufficiently large to ignore its curvature compared to a single water molecule, the average number of electrons transferred to the sp^2 network during its interaction with a single water molecule was calculated to be 0.001 and 0.016 electrons for the pristine and ECO-treated coiled CNT yarns, respectively. Figure 1c-(i) and Figure 1c-(ii) show images for visualizing the

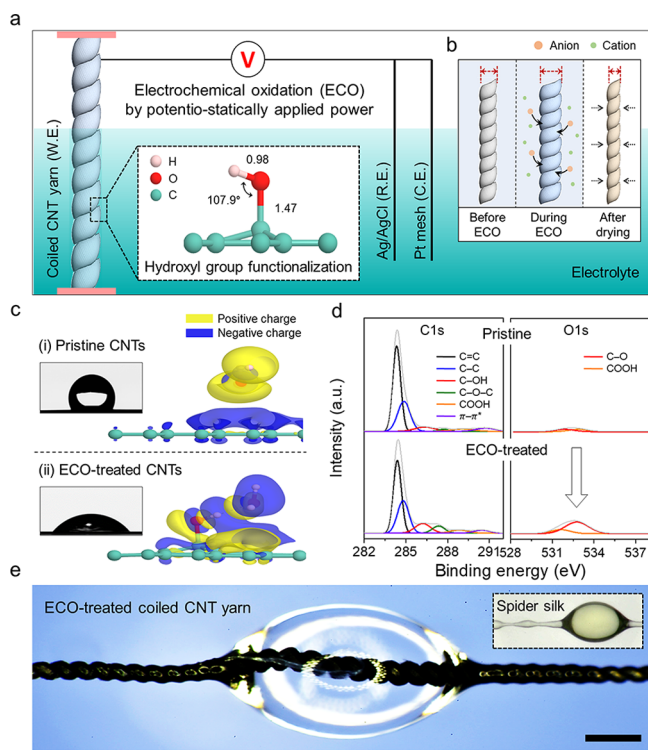


Figure 1. Extrinsic hydrophilicity of the coiled carbon nanotube (CNT) yarns induced by electrochemical oxidation (ECO). (a) Schematic illustration showing the experimental setup for the ECO treatment using a three-electrode system consisting of coiled CNT yarns (the working electrode), Ag/AgCl (the reference electrode), Pt mesh (the counter electrode), and 0.1 M Na₂SO₄ (the electrolyte). Inset: Schematic of the molecular structure of the functionalized hydroxyl groups in the C=C bond sp² network. (b) Schematics showing the volume expansion of a coiled CNT yarn by charge injection during electrochemical oxidation (ECO) and the reduction in yarn diameter after drying. (c) Visualized charge transfer reaction from a water molecule to (i) pristine and (ii) ECO-treated CNTs with the isosurface of level 0.0003 e Å⁻³. Yellow and blue colors represent positive and negative charge, respectively. Insets: Contact angle measurements between a water droplet and the CNT sheet stack before and after ECO treatment. (d) C 1s and O 1s XPS analysis spectra of the pristine (upper) and ECO-treated coiled CNT (lower) yarns. (e) Photograph showing a water droplet absorbed onto the middle of the ECO-treated coiled CNT yarn (scale bar = 1 mm). Inset: Image of water droplets on spider silk as a comparison.⁵⁸

charge transfer mapping of water molecule adsorption to the sp² network for pristine and ECO-treated CNT yarns, respectively. The mapping images reveal that a stronger interaction between the charge-polarized hydroxyl-modulated surface and polar water molecules results in stronger charge transfer between water and ECO-treated CNTs; therefore, the binding energy for water molecules drastically increases from 0.021 to 0.221 eV. These results support that the ECO-treated CNTs are more hydrophilic and exhibit substantially higher wettability and water interactivity. The electrochemical treatment surface oxidation effect on the hydrophobicity/hydrophilicity of the CNT yarns was also verified through contact angle measurement between water droplets and the CNT surface. The water contact angle on the pristine CNT sheet stack was measured to be 118°, which was reduced to 40° after ECO treatment (the insets in Figure 1c). Additionally, the ECO-treated coiled CNT yarns were fully hydrated after

immersion in water, while the pristine coiled CNT yarn did not exhibit any proof of wettability (Figure S3).

Oxidation time, corresponding to the plateau region of the current density plot, was defined as T_{ECO} for the treatment under constant voltage. It was found that the T_{ECO} could provide information on the optimized oxidation time (~10 s) for a given applied voltage (~4.5 V vs Ag/AgCl). Therefore, we usually terminated the ECO treatment reaction at T_{ECO} for normal oxidation (Figure S4). Unless otherwise stated, most ECO treatments performed under constant voltage of 4.5 V (vs Ag/AgCl) for 10 s. T_{ECO} is inversely proportional to the applied voltage; therefore, it increased from 15 to 30 s when the applied voltage was reduced from 4.0 to 3.0 V (vs Ag/AgCl) (Figure S5). The following drop in current density beyond the T_{ECO} region may be attributed to the excessive creation of oxygen-containing functional groups due to severe oxidation, which increased the yarn resistance from 0.021 to 90 kΩ/cm by disrupting π-π conjugation. Plots of applied voltage versus maximum current, oxidation time, input electrical power, and resultant input energy are shown in Figure S6. Notably, the total input energy (approximately 2.6 J/cm) required for ECO treatment was approximately constant at given voltages, which is significantly less^{46–48} than previously reported plasma-based results. The degree of oxidation of the coiled CNT yarns was largely adjusted by changing the oxidation time or applied voltage (vs Ag/AgCl). The results of X-ray photoelectron spectroscopy (XPS) and Raman spectroscopy analyses demonstrate the changes in the coiled CNT yarns before and after ECO treatment. As shown in the XPS spectra, there are two dominant photoemission peaks of C 1s (284 eV) and O 1s (533 eV). The CNT yarns were oxidized at various voltages (3.0–4.5 V vs Ag/AgCl) and application time (up to 30 s), and the resulting XPS peaks and oxygen/carbon (O/C) atomic ratios are plotted in Figure S7. Although the degree of oxidation is roughly proportional to the applied voltage or oxidation time, the final O/C ratios tend to converge at approximately 0.26, indicating the successful functionalization of the oxygen-containing groups on the CNT surface. The ratio of the intensities of the D and G bands (I_D/I_G) from the Raman spectra (Figure S8)—representing the degree of the atomic defect—also increased from 0.49 to 0.79 via ECO treatment, thereby supporting the XPS results. Additionally, the high-resolution XPS spectra for C 1s (left panel of Figure 1d) and O 1s (right panel of Figure 1d) binding energy in the ECO-treated coiled CNT yarns revealed the specific functional group types and amounts. After deconvolution using Gaussian peak fitting, the high-resolution C 1s spectra showed noticeable peaks at 284.4 and 284.9 eV, representing C=C sp² and C-C sp³ bonds, respectively. Moreover, several oxygen-containing functional groups—hydroxyl (C-OH), epoxy (C-O-C), and carboxylic (COOH)—were located at 286.1, 287.4, and 288.8 eV, respectively (Table S1). The O 1s spectra also contained peaks for C-O (532.8 eV) and COOH (531.6 eV) bonds. These results are consistent with previous studies.⁴⁹ Although the oxygen content found in the XPS spectrum of pristine CNT was negligible, the peak values of oxygen functional groups for the ECO-treated CNT yarns became noticeably more enhanced as the ECO treatment proceeded. In addition, Fourier-transform infrared (FTIR) spectra also confirmed the existence of these functional groups, showing consistency with the XPS results (Figure S9). Among the various types of oxygen functional groups, C-OH was mainly detected,

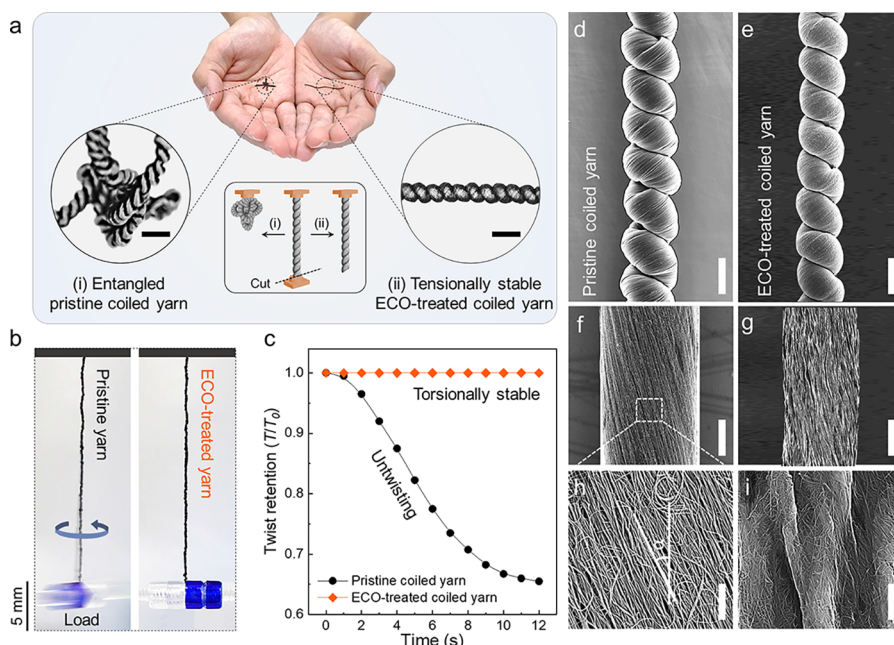


Figure 2. Structural stability and morphological characterization of the ECO-treated coiled carbon nanotube (CNT) yarns. (a) Photograph of (i) entangled pristine coiled yarn and (ii) tensionally stable ECO-treated coiled yarn placed on both palms, respectively, and optical images of its magnification (scale bars = 300 μm). Inset: Schematic illustrations showing the morphological change of (i) pristine and (ii) ECO-treated coiled CNT yarns when one end of the yarns is cut, respectively. (b) Photographs showing vigorous untwisting of pristine coiled yarns (left) and twist-stability of the ECO-treated coiled yarn (right) after the release of tethering of a 190-kPa freely rotating load, respectively. (c) The time dependence of twist retention was recorded upon release of the tethering for pristine coiled yarns (black circle) and ECO-treated coiled yarns (orange diamond). Scanning electron microscopy (SEM) images of (d) a pristine and (e) an ECO-treated coiled yarn before applying a freely rotating load (scale bar = 150 μm). (f,g) SEM images and (h,i) magnified SEM images of a twisted pristine yarn (f,h) before and (g,i) after ECO treatment and drying, indicating a large diameter reduction, microbuckling on the yarn surface, and an approximately zero bias angle state (scale bar: (f,g) = 80 μm and (h,i) = 2 μm). The definition of the yarn bias angle (α) for the pristine yarns is denoted in panel h.

followed by C–O–C and COOH in the ECO-treated CNT yarns. Therefore, C–OH is the critical component contributing to the extrinsic hydrophilicity of the ECO-treated coiled CNT yarns.

The water droplet was well absorbed and hung onto the ECO-treated coiled CNT yarn due to the extrinsic hydrophilicity (Figure 1e). The yarn is reminiscent of its naturally hydrophilic counterpart, spider silk, which can effectively collect and harvest water droplets when the dew point changes in the early morning (see inset of Figure 1e).⁵⁸ The nanoscale helical gaps between the CNT fibrils of the pristine CNT yarns can provide a capillary effect for effective and fast solvent absorption.¹¹ Hence, the ECO-treated coiled CNT yarns also exhibited fast, reversible, and large volume expansion (60% on average) after repeated water absorption cycles (Figure S10). Furthermore, the notable experimental proof for the extrinsic hydrophilicity was obtained by investigating the hydration-driven mechanical actuation of the ECO-treated coiled yarns because they could generate contractile tensile actuation by increasing yarn volume, as previously reported.^{9,14,16} Fast infiltration into the dried ECO-treated coiled CNT yarn resulted in the maximum tensile contraction of 10.5% (under a load of 290 kPa) when it was brought into contact with water, whereas the pristine coiled CNT yarn did not show any signs of wettability and tensile actuation (Figure S11).

Structural Stability of Resulting ECO-Treated Coiled CNT Yarns. Coiled CNT yarns have great advantages for diverse wearable applications; however, structural stability during the handling of such coiled yarns is a key issue.¹⁵ Figure

2a and its inset show the morphological differences of the pristine and ECO-treated coiled CNT yarns when one or both ends of the yarns are cut, respectively. Generally, pristine coiled CNT yarns are prone to vigorous untwisting,²⁹ rapid entanglement, or snarling⁸ when one end becomes untethered due to the highly applied torsional stress, which was also observed in our experiments (see Movie S1). Therefore, both ends of the coiled yarn should always be tethered to keep it in the coiled state. Such structural collapse of the coil is one of its limitations when used in real applications. On the contrary, the ECO-treated coiled CNT yarns can stabilize their highly inserted twists even in the free-standing state. The ECO-treated coiled CNT yarns retained their coil morphology in a free-standing (self-supporting) state even when one end of the yarn was cut, showing no entanglement or snarling with pristine coiled CNT yarn (Movie S2). Additionally, the ECO-treated coiled yarns negligibly untwisted and remained straight even upon the release of tethering of a 190 kPa freely rotating load (right side), unlike the rapidly rotating pristine coiled yarn (left side) (Figure 2b). In other words, the inserted twists in the ECO-treated coiled yarn were largely retained while the inserted twists in the pristine coiled yarn reduced drastically. A comparison of twist retention performance of pristine and ECO-treated coiled yarns versus time is presented in Figure 2c. The ECO-treated coiled yarn showed 92% twist retention, whereas the pristine coiled yarn showed only 65% twist retention when both yarns were not tethered. This twist-stability can be advantageous in stretchable electrical conductors. The resulting coiled yarn exhibited about 110%

fracture strain with a tensile strength of 36.4 MPa; however, we used 80% as the maximum strain limit for the stable and reversible mechanical or electrical performance. The modulus for the yarn was 29.7 MPa, which is similar to the previously reported values for spring-like CNT ropes (33 MPa) (Figure S12).⁷ In general, a normally coiled CNT yarn undergoes a large resistance change (68% at 80% strain) due to coil opening during stretching (Figure S13). However, the resistance changes in the ECO-treated coiled CNT yarn can be reduced by designing the coils to have a certain distance between the loops (19% at 80% strain). Therefore, the open-loop shape becomes memorized; hence, the ECO-treated coiled CNT yarns can provide lower resistance changes than the pristine coiled CNT yarn. This ECO-driven twist-stability can be applied to other coiled CNT yarn-based devices, such as artificial muscles^{9,17,59} and stretchable conductors.⁷

We observed the microstructure change of the pristine coiled yarns before and after ECO treatment through scanning electron microscopy (SEM) images to clarify the origin of this twist-stability (Figure 2d,e, and Figure S14). The as-twisted CNT yarns with a constant bias angle reminiscent of a one-chirality McKibben structure⁶⁰ were overtwisted (5500 turns m⁻¹); they formed dense coil loops (55 coils/cm) with a coil index (the coil diameter divided by the yarn diameter) of 1.48, as shown in Figure 2d. The yarn retained a uniform coil structure similar to the pristine coiled yarn after ECO treatment and drying (Figure 2e). However, it exhibited completely different morphological transitions, including a large diameter reduction (11.5%), microbuckling on the yarn surface, and an approximately zero bias angle state (Figure S14). Consistent results were more evidently revealed when applying the ECO treatment to pristine noncoiled CNT yarns. The fibrils of presented yarn exhibited a highly aligned structure with a bias angle of 25° with respect to the yarn direction (Figure 2f) when 600 turns m⁻¹ of twist was applied, which was largely related with the following equation: $\alpha = \tan^{-1}(2\pi rT)$, where α , r , and T represent the bias angle, radius, and the number of twists, respectively.⁶⁰ The outer diameter of the CNT yarn measured from the SEM images (Figure 2f,g) decreased from approximately 235 μm to 165 μm, corresponding to the drastic increase in average yarn density (105%). High-magnification SEM images showed the increment of internanotube connections and the condensed nanotube bundle with surface buckling, implying a reduction of nanotube interspace in the yarn (Figure 2h,i).

These obvious morphological changes driven by ECO treatment cannot be explained by just a simple surface tension effect due to the drying of injected water. One possibility is that electrochemical charge injection during ECO treatment produces unexpectedly large volume expansion (125%), as mentioned earlier. The charge injection is expected to increase an internal pressure for a heavily twisted CNT yarn half-infiltrated by the electrolyte that results in volume expansion of the yarn. The CNT yarn volume change is highly correlated with the torsional and tensile actuation when the electrochemical voltage is applied as long as a one-chiral McKibben structure is maintained: a 1% increase in yarn length introduced a 3.2% decrement in yarn volume.⁶⁰ However, the present coiled CNT yarn was experimentally two-end tethered and fully infiltrated by electrolyte during the oxidation; therefore, neither torsional nor tensile actuation could occur.^{60,61} Hence, the internal pressure relaxation was completely converted into a much larger volume expansion

than usual because volume expansion was the only way to relax the internal pressure without producing either type of actuation. Possible partial collapse of the McKibben structure initialized the bias angle during the marked volume expansion of the CNT yarn. Moreover, yarn shrinkage from this largely expanded state during yarn drying led to surface buckling (Figure 2i). The microstructural transition after the ECO-driven marked volume expansion relaxed the initially introduced torsional stress, as evidenced by initialization of the bias angle; the approximately zero bias angle implies that the coiled CNT yarn had approximately no driving force to start the untwisting or entanglement in the free-standing state.

Electrochemical Performance Characterization and Wearable Supercapacitors Demonstration.

It is necessary to assign mechanical stretchability to the CNT yarn-based energy storage devices based on the target application of a power source for wearable electronics because the human motion generates a maximum of 50% strain during physical activity.⁶² In previous work, our group suggested that yarn-coiling is a simple but powerful strategy for assigning extrinsic stretchability to intrinsically nonstretchable yarns or fibers.^{20,22} However, coiling the yarns or fibers requires high tensile or torsional toughness to withstand the severe deformation generated during overtwisting. Therefore, yarn fracturing before coiling must be avoided in CNT yarn electrodes loaded with a high wt % of pseudocapacitive materials.²⁴

The proposed ECO-treated coiled CNT yarn can serve as effective electrodes while constructing advanced electrochemical energy storage systems having high capacitance and stretchability. The electrochemical performances of the pristine and ECO-treated coiled CNT yarns were characterized and compared using a three-electrode system. Cyclic voltammetry (CV) plots for supercapacitors fabricated with ECO-treated coiled CNT yarns with different treatment times were also compared (Figure 3a). The area under the curve (AUC) of the CV plot increased dramatically with increasing oxidation time: an approximately 17-fold larger AUC of the CV plot than that of the supercapacitor fabricated with pristine coiled CNT yarns was obtained after applying 4.5 V (vs Ag/AgCl) for 10 s. A similar increasing AUC trend was also observed for various applied voltages of 3.0, 3.5, and 4.0 V (vs Ag/AgCl) (Figure S15). The capacitance enhancement ratio—the CV AUC ratio before and after ECO treatment—versus T_{ECO} is plotted for various applied voltages, as shown in Figure S16. It should be noted that irrespective of applied voltage in a given range, ECO treatment caused the capacitance enhancement ratios to converge at an approximately 17-fold enhancement.

Supercapacitors consisting of symmetrical two parallel-structured ECO-treated coiled CNT yarns were prepared, and their electrochemical performances were characterized. The box-like rectangular CV curves (scan rates from 10 to 100 mV/s) of the ECO-treated coiled yarn electrode clearly show the absence of faradaic redox reactions, which is consistent with the energy storage mechanism due to the EDLC of the CNT yarns and the pseudocapacitance of the oxygen-containing groups (Figure 3b). Mechanical properties and equivalent series resistance were roughly maintained because of achieving the effective capacitance improvement through the ECO treatment (Figure S17). The rectangular-like CV curve was roughly maintained at scan rates of up to 1000 mV/s, showing the relatively high rate capability of the present ECO-treated coiled CNT yarn supercapacitor (Figure S18); such a high rate capability is advantageous for those applications that

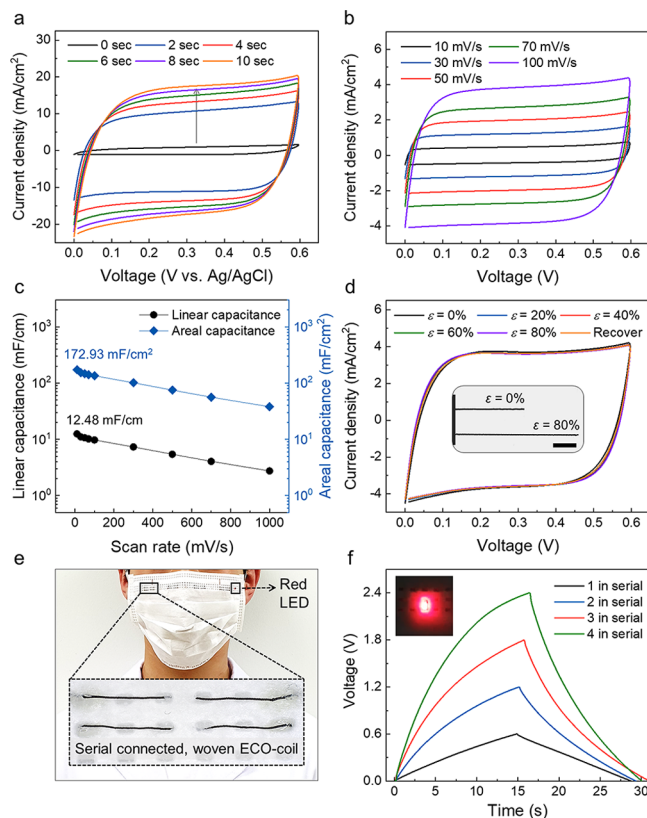


Figure 3. Electrochemical performance of the assembled stretchable supercapacitors and demonstration as a wearable power source. (a) Cyclic voltammetry (CV) curves (at 10 mV/s) were measured in a three-electrode system and compared for the electrochemical oxidation (ECO)-treated coiled carbon nanotube (CNT) yarns for various periods (0–10 s) at a given voltage of 4.5 V (vs Ag/AgCl). (b) CV curves at scan rates (10–100 mV/s). The measurements were performed with a two-electrode system consisting of two symmetrical ECO-treated coiled CNT yarn electrodes. (c) Calculated single-electrode linear (black circle) and areal (blue diamond) capacitance values of ECO-treated coiled yarn supercapacitors at scan rates from 10 to 1000 mV/s. (d) CV curves for the applied static strain from 0% to 80% and the recovered state of the ECO-treated coiled yarn supercapacitor. Inset: optical image of an ECO-treated coiled CNT yarn before and after $\epsilon = 80\%$ (scale bar = 3 mm). Optical images showing (e) four serially connected PVA/LiCl quasi-solid-state electrolyte-coated, ECO-treated coiled yarn supercapacitors sewn into a commercialized mask. (f) Galvanostatic charge/discharge curves were obtained from supercapacitors sewn into the mask (current density = 1.84 mA/cm²). The inset image shows a red light-emitting diode (LED) powered by the mask.

require high power (such as artificial muscles) compared to transition metal oxide-based pseudocapacitive supercapacitors that show distorted curves at high scan rates due to their poor electrical properties.^{24,53} The maximum linear and areal capacitance values of the ECO-treated coiled CNT yarn supercapacitors versus the scan rate were calculated from the CV curves at 10 mV s⁻¹ to be 12.48 mF cm⁻¹ and 172.93 mF cm⁻² (based on single electrode capacitance), respectively (Figure 3c). Figure S19 shows the capacitance retention performance of the ECO-treated coiled CNT yarn supercapacitor for repeated charge/discharge cycles. The initial capacitance was retained approximately at 91% after 1000 cycles with stable EDLC-like properties.

The CV curves for the yarn supercapacitors were measured while statically applying various strains to investigate the effects of mechanical tensile strains on the charge storage capability of the ECO-treated coiled CNT yarn supercapacitor (Figure 3d). The corresponding capacitance retention versus strain for the ECO-treated coiled CNT yarn supercapacitor and its cycle performance against repeated stretch/release deformations are shown in Figure S20. Although the above areal capacitance (172.93 mF cm⁻²) for the present yarn supercapacitors is lower than that of nitrogen-doped graphene fiber supercapacitors,⁶³ our stretchability (80%) is much higher (Table S2). Using the ECO-coil supercapacitors as a wearable power source demonstrated its practical strength and toughness when woven into a commercially available mask (Figure 3e). Four ECO-treated coiled CNT yarn supercapacitors were woven into the mask, and connected serially and coated with quasi-solid-state poly(vinyl alcohol) (PVA)-LiCl gel electrolyte to complete the mask-based supercapacitor (Figure S21). Considering the volatility of the gel electrolyte and the safety for humans, we encapsulated the mask supercapacitor by coating Ecoflex 00-30 materials. As a result, the encapsulated mask supercapacitor exhibited stable electrochemical performance with a capacitance retention of 95% (at 100 mV/s) over 2 weeks (Figure S22). We plot galvanostatically measured voltage–time curves for the woven supercapacitors (Figure 3f). Both triangular-shaped curves and proportional peak voltage increased with the number of serially connected supercapacitors, indicating stable charge storage performance. Finally, a red light-emitting diode (LED) was powered by the mask supercapacitor (inset of Figure 3f), and its brightness can be further enhanced by connecting more supercapacitors.

Origin of the Capacitance Improvement. The possible origin of capacitance improvement by ECO treatment can be categorized into several parts. First, improved wettability can induce effective charge transfer from water molecules to the ECO-treated coiled CNT surface, providing high accessibility to hydrated ions in the electrical double-layer.⁴⁸ Second, oxygen-containing functional groups can act as electrochemically active sites for pseudocapacitive reactions.^{64,65} Especially, hydroxyl and carboxy groups are reported to have a high pseudocapacitive effect by providing successive redox mechanisms.⁶⁶ The reversible and fast ion adsorption/desorption on these oxygen-containing groups can dramatically enhance the specific capacitance over the electrical double layer capacitance (EDLC) of pure CNTs.⁶⁷ Third, the increased surface area by yarn volume expansion and surface buckling also provides more electrochemically active sites for a given unit area or length of the yarn. Finally, enhanced quantum capacitance (C_Q) due to oxygen-containing groups can improve the capacitance. It has been reported that the density of state (DOS) provides room for transferred electrons from ion adsorption. Therefore, it can be a critical factor for determining the charge storage capacity of EDLC,⁶⁸ especially for atomistically thin electrodes.

Figure 4a–c and inset therein show calculated DOS of the oxygen-containing functional groups and the atomic structure, respectively. The pristine sp²-carbon network has a valley-like DOS near the Fermi level. Once the hydroxyl or epoxy groups were functionalized, additional DOS was introduced near the Fermi level. The quantum capacitance was drastically enhanced because the energy state of the hydroxyl group was closer to the Fermi level (see Figure 4d). This additional DOS of the electrode plays a key role in storing charge from

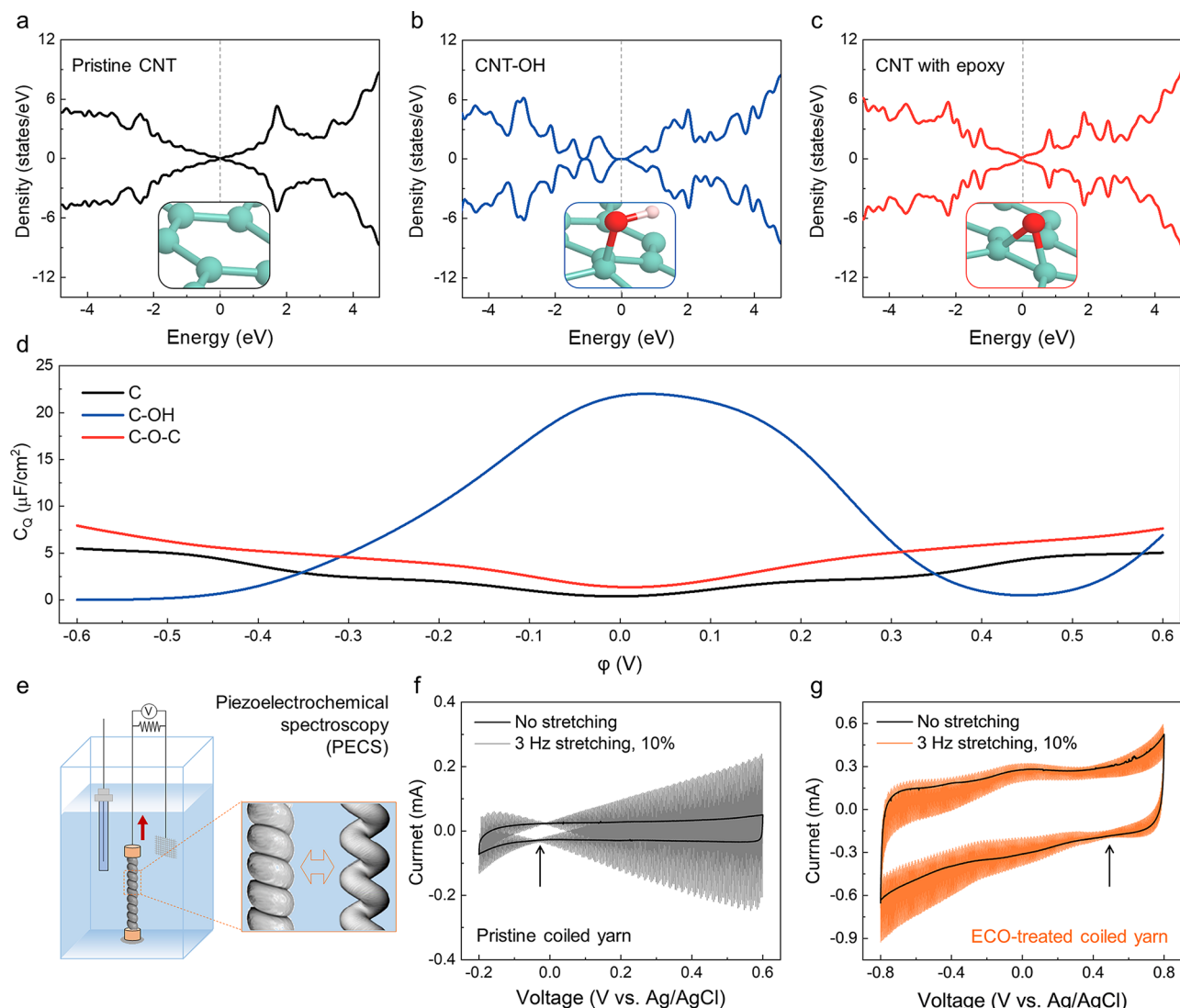


Figure 4. Origin of the capacitance enhancement. The calculated density of state (DOS) for (a) a pristine CNT, (b) a hydroxyl group, and (c) an epoxy group on a functionalized ECO-treated CNT surface. Inset schematic images from panels a, b, and c show atomic structures of a pristine CNT, a hydroxyl group, and an epoxy group on a functionalized ECO-treated CNT surface, respectively. (d) Calculated quantum capacitance values for a pristine CNT, a hydroxyl group, and an epoxy group on a functionalized ECO-treated CNT surface. (e) A schematic illustration showing the experimental setup for piezoelectrochemical spectroscopy (PECS) consisting of coiled CNT yarns (the working electrode), Ag/AgCl (the reference electrode), and Pt mesh (the counter electrode) immersed in 0.1 M Na_2SO_4 (the electrolyte). Measured PECS curves for (f) pristine and (g) ECO-treated coiled CNT yarns with an applied strain and deformation frequency of 10% and 3 Hz, respectively. The expected potential of zero charge (PZC) is denoted by the arrows in panels f and g, respectively.

reversible ion adsorption–desorption during supercapacitor operation. On the other hand, the energy state of the epoxy-functional group was 1 eV away from the Fermi level; hence, the enhancement was not as dominant as that bestowed by the hydroxyl groups.

The potential of zero charge (PZC) for evaluating the equilibrium charge state was investigated to further confirm the hydroxyl groups as the origin of the enhanced capacitance by piezoelectric spectroscopy (PECS),⁶⁹ which can provide an insight into the surface functionalization *via* the ECO treatment. A coiled CNT yarn in the three-electrode system can be cyclically stretched by up to 10% and recover sinusoidally with 3 Hz according to dynamic measurements using CV curves (Figure 4e). PZC—the corresponding potential at which the AC current is minimized—and current phase inversion by 180° were located at approximately 0 V (vs

Ag/AgCl) for the pristine coiled CNT yarn (Figure 4f). On the other hand, a possible PZC point for the ECO-treated coiled CNT yarn was located at approximately 0.45 V (vs Ag/AgCl) in the extended voltage window, as shown in Figure 4g. The shift in PZC for the ECO-treated coiled CNT yarn along the positive voltage direction can be due to the negatively charged hydroxyl groups created during the functionalization. Hence, the formation of hydroxyl groups *via* ECO treatment is a key factor for enhancing the capacitance performance.

CONCLUSIONS

In summary, we report twist-stable and hydrophilic coiled CNT yarns that have oxygen-containing functional groups *via* a simple and cost/energy effective ECO treatment. Originating from the morphological transitions of the coiled CNT yarn after the ECO-driven large volume expansion, extraordinary

twist-stability was obtained even when torsional rotors were deployed. Another highlight of ECO-treated coiled yarn is its possible application to advanced electrodes for high-performance electrochemical energy storage systems with high storage capability and stretchability. The ECO-treated coiled yarn supercapacitor showed an improved capacitance (approximately 17-fold) with high stretching tolerance (up to 80%), benefiting from enhanced wettability and quantum capacitance. Moreover, extrinsically bestowed hydrophilicity enabled large and fast hydro-volume expansion upon exposure to water. Therefore, water/humidity-driven smart artificial muscles with high energy and power densities are one of the suggested applications of the ECO-treated coiled CNT yarn. On the basis of these demonstrations, the ECO-induced twist-stability and hydrophilicity characteristics can become a universally applicable strategy for coiling-based CNT yarns in robotic arms, stretchable electrical conductors, and energy harvesters to achieve practical wearable devices.

EXPERIMENTAL SECTION

Preparation of Pristine Coiled CNT Yarns. Ten layers of CNT sheets drawn from a 320- μm high CNT forest (A-Tech System Co., Korea) were assembled into a 20 mm-wide and 100 mm-long sheet stack. Each end of the stacked sheet was attached to two pieces of adhesive carbon tape for cone spinning, and then it was manually rolled into a \sim 3 mm-diameter cylinder. The CNT cylinder was then suspended vertically on the motor tip end with a load of \sim 3.5 g for coil twisting. The pristine coiled CNT yarns were fabricated by inserting a giant twist (\sim 5500 turns m^{-1}) into the cylinder. After that, the coiled yarns were cut into 1.0 cm-long pieces and electrically connected to a 190 μm diameter Cu wire using silver paste for ECO treatment and electrochemical performance characterization.

Preparation of Mask Supercapacitors. The PVA-LiCl gel electrolyte was prepared by heating a mixture of 3 g of PVA (MW, 146 000–186 000) and 6 g of LiCl in 30 mL of deionized water at 90 °C for several hours until it became transparent. The woven mask supercapacitors were made by weaving ECO-treated coiled CNT yarns into a mask using a needle. The yarns were then coated with the PVA-LiCl gel electrolyte and encapsulated with Ecoflex 00-30 (Smooth-On, Inc.) materials. The chemicals for electrolyte synthesis were purchased from Sigma-Aldrich.

Characterization. SEM and optical images were obtained using an S-4600 (Hitachi, Japan) and D750 (Nikon, Japan) instrument, respectively. X-ray photoelectron spectroscopy (XPS) measurements were performed on an ESCALAB 250XI (Thermo Scientific) instrument. In the testing of strain sensing, the yarns were mounted on digital Vernier calipers (Mitutoyo, Japan) with both their ends electrically connected to multimeter probes (15+, Fluke). The ECO treatment was conducted in a typical three-electrode configuration with coiled CNT yarns as the working electrode, an Ag/AgCl electrode as the reference electrode, Pt mesh as the counter electrode, and 0.1 M Na₂SO₄ aqueous solution as the electrolyte. All of the electrochemical tests were performed using an electrochemical analyzer (Vertex EIS, Ivium) to calculate the specific capacitance values of the coiled CNT yarn supercapacitors. The capacitance of a single electrode in the coiled yarn supercapacitors was calculated from CV curves using $C = I/(dV/dt)$, where I is the average discharge current and the dV/dt denotes the scan rate. The specific areal capacitance (C_{sp}) was calculated by applying eq 1:

$$C_{\text{sp}}(\text{F/cm}^2) = 2C/A_{\text{surface}} \quad (1)$$

where A_{surface} represents the total external surface area of the coiled CNT yarn. The total length and volume of the coiled CNT yarn were used for the linear and volumetric capacitance calculations, respectively.

Computational Details. DFT calculations were performed using the Vienna *ab initio* simulation package⁷⁰ and the projector

augmented wave potential.⁷¹ The Perdew–Burke–Ernzerhof⁷² exchange-correlation functional was used to assess the precision of the implementation. A 4×4 monolayer graphene sheet model with 32 carbon atoms was constructed to simplify the structure of pristine CNT. A Γ -centered k -points mesh of $4 \times 4 \times 1$ was employed to sample the two-dimensional Brillouin zone. The plane-wave energy cutoff was set to 520 eV, and Hellmann–Feynman forces were under 0.01 eV/Å. The Bader method⁷³ was used to analyze the average charge transfer between water molecules and either pristine or hydroxyl group functionalized graphene. The differential charge densities were defined as in eq 2:

$$\Delta\rho(r) = \rho_{\text{tot}}(r) - \rho_{\text{gra}}(r) - \rho_{\text{H}_2\text{O}}(r) \quad (2)$$

where $\rho_{\text{tot}}(r)$ represents the total electronic density of the water molecule/graphene system and $\rho_{\text{gra}}(r)$ and $\rho_{\text{H}_2\text{O}}(r)$ are the densities for the isolated pristine graphene or hydroxyl group functionalized graphene and water molecules, respectively. The quantum capacitance was calculated using eq 3:

$$C_Q = \frac{e^2}{4kT} \int_{-\infty}^{\infty} D(E) \operatorname{sech}^2\left(\frac{E + e\phi}{2kT}\right) dE \quad (3)$$

where $k = 8.617 \text{ eV/K}$ is the Boltzmann constant, T denotes the room temperature, $e = 1.602 \times 10^{-19} \text{ C}$ is the elementary charge, $D(E)$ represents the density of states of the supercell system, $f(E)$ is the Fermi–Dirac distribution function, and E is the energy relative to E_F .

ASSOCIATED CONTENT

SI Supporting Information

The Supporting Information is available free of charge at <https://pubs.acs.org/doi/10.1021/acsnano.1c09465>.

Fabrication of coiled CNT yarns; photograph of experimental setup for ECO treatment; optical images and SEM images of pristine coiled CNT yarns and ECO-treated coiled CNT yarns; ECO treatment characterizations with various applied voltages; surface analysis of CNT yarns before and after ECO treatment by XPS, Raman, and FTIR spectra; hydro-volume changes and tensile stroke measurements for ECO-treated coiled CNT yarns; mechanical, electrical, and electrochemical properties of ECO-treated coiled CNT yarns (PDF)

Entangled pristine coiled CNT yarn when one end was cut (MP4)

Free-standing ECO-treated coiled CNT yarn when one end was cut (MP4)

AUTHOR INFORMATION

Corresponding Authors

Dongseok Suh – Department of Energy Science, Sungkyunkwan University, Suwon 16419, Republic of Korea; [ORCID iD](https://orcid.org/0000-0002-0392-3391); Email: energy.suh@skku.edu

Changsoon Choi – Department of Energy and Materials Engineering, Dongguk University-Seoul, Seoul 04620, Republic of Korea; [ORCID iD](https://orcid.org/0000-0003-4456-4548); Email: cschoi84@dongguk.edu

Authors

Wonkyeong Son – Department of Energy and Materials Engineering, Dongguk University-Seoul, Seoul 04620, Republic of Korea; Department of Energy Science, Sungkyunkwan University, Suwon 16419, Republic of Korea

Sungwoo Chun – Department of Electronics and Information Engineering, Korea University, Sejong 30019, Republic of Korea

Jae Myeong Lee – Department of Energy and Materials Engineering, Dongguk University-Seoul, Seoul 04620, Republic of Korea

Gichan Jeon – Department of Energy and Materials Engineering, Dongguk University-Seoul, Seoul 04620, Republic of Korea

Hyeon Jun Sim – Department of Energy and Materials Engineering, Dongguk University-Seoul, Seoul 04620, Republic of Korea

Hyeon Woo Kim – Convergence Technology Division, Korea Institute of Ceramic Engineering and Technology (KICET), Jinju-si 52851, Republic of Korea

Sung Beom Cho – Convergence Technology Division, Korea Institute of Ceramic Engineering and Technology (KICET), Jinju-si 52851, Republic of Korea; orcid.org/0000-0002-3151-0113

Dongyun Lee – Department of Nanoenergy Engineering, Pusan National University, Busan 46241, Republic of Korea

Junyoung Park – Department of Energy and Advanced Material Engineering, Dongguk University-Seoul, Seoul 04620, Republic of Korea

Joonhyeon Jeon – Division of Electronics & Electronical Engineering, Dongguk University-Seoul, Seoul 04620, Republic of Korea

Complete contact information is available at:

<https://pubs.acs.org/10.1021/acsnano.1c09465>

Author Contributions

W.S. and S.C. contributed equally to this work. W.S., S.C., D.S., H.S., and C.C. conceived the idea and performed the experiments. J.M.L., G.J., J.J., and D.L. analyzed the experimental results. H.W.K., J.P., and S.B.C. performed the simulation works. All authors contributed to writing the manuscript.

Notes

The authors declare no competing financial interest.

ACKNOWLEDGMENTS

This work was supported by Korea Institute of Energy Technology Evaluation and Planning (KETEP) and the Ministry of Trade, Industry & Energy (MOTIE) of the Republic of Korea (No. 20194030202320) and the Basic Science Research Programs through the National Research Foundation of Korea (NRF-2021R1A2C2005281).

REFERENCES

- (1) Zhang, M.; Atkinson, K. R.; Baughman, R. H. Multifunctional Carbon Nanotube Yarns by Downsizing an Ancient Technology. *Science* **2004**, *306*, 1358–1361.
- (2) Koziol, K.; Vilatela, J.; Moisala, A.; Motta, M.; Cunniff, P.; Sennett, M.; Windle, A. High-Performance Carbon Nanotube Fiber. *Science* **2007**, *318*, 1892–1895.
- (3) Zhang, X.; Jiang, K.; Feng, C.; Liu, P.; Zhang, L.; Kong, J.; Zhang, T.; Li, Q.; Fan, S. Spinning and Processing Continuous Yarns from 4-Inch Wafer Scale Super-Aligned Carbon Nanotube Arrays. *Adv. Mater.* **2006**, *18*, 1505–1510.
- (4) Randeniya, L. K.; Bendavid, A.; Martin, P. J.; Tran, C.-D. Composite Yarns of Multiwalled Carbon Nanotubes with Metallic Electrical Conductivity. *Small* **2010**, *6*, 1806–1811.

(5) Jiang, K.; Li, Q.; Fan, S. Spinning Continuous Carbon Nanotube Yarns. *Nature* **2002**, *419*, 801.

(6) Li, Y.-L.; Kinloch, I. A.; Windle, A. H. Direct Spinning of Carbon Nanotube Fibers from Chemical Vapor Deposition Synthesis. *Science* **2004**, *304*, 276–278.

(7) Shang, Y.; He, X.; Li, Y.; Zhang, L.; Li, Z.; Ji, C.; Shi, E.; Li, P.; Zhu, K.; Peng, Q.; Wang, C.; Zhang, X.; Wang, R.; Wei, J.; Wang, K.; Zhu, H.; Wu, D.; Cao, A. Super-Stretchable Spring-Like Carbon Nanotube Ropes. *Adv. Mater.* **2012**, *24*, 2896–2900.

(8) Shang, Y.; Li, Y.; He, X.; Du, S.; Zhang, L.; Shi, E.; Wu, S.; Li, Z.; Li, P.; Wei, J.; Wang, K.; Zhu, H.; Wu, D.; Cao, A. Highly Twisted Double-Helix Carbon Nanotube Yarns. *ACS Nano* **2013**, *7*, 1446–1453.

(9) Lima, M. D.; Li, N.; de Andrade, M. J.; Fang, S.; Oh, J.; Spinks, G. M.; Kozlov, M. E.; Haines, C. S.; Suh, D.; Foroughi, J.; Kim, S. J.; Chen, Y.; Ware, T.; Shin, M. K.; Machado, L. D.; Fonseca, A. F.; Madden, J. D. W.; Voit, W. E.; Galvão, D. S.; Baughman, R. H. Electrically, Chemically, and Photonically Powered Torsional and Tensile Actuation of Hybrid Carbon Nanotube Yarn Muscles. *Science* **2012**, *338*, 928–932.

(10) Kim, S. H.; Lima, M. D.; Kozlov, M. E.; Haines, C. S.; Spinks, G. M.; Aziz, S.; Choi, C.; Sim, H. J.; Wang, X.; Lu, H.; Qian, D.; Madden, J. D. W.; Baughman, R. H.; Kim, S. J. Harvesting Temperature Fluctuations as Electrical Energy using Torsional and Tensile Polymer Muscles. *Energy Environ. Sci.* **2015**, *8*, 3336–3344.

(11) Chen, P.; Xu, Y.; He, S.; Sun, X.; Pan, S.; Deng, J.; Chen, D.; Peng, H. Hierarchically Arranged Helical Fibre Actuators Driven by Solvents and Vapours. *Nat. Nanotechnol.* **2015**, *10*, 1077–1083.

(12) Di, J.; Fang, S.; Moura, F. A.; Galvão, D. S.; Bykova, J.; Aliev, A.; de Andrade, M. J.; Lepró, X.; Li, N.; Haines, C.; Ovalle-Robles, R.; Qian, D.; Baughman, R. H. Strong, Twist-Stable Carbon Nanotube Yarns and Muscles by Tension Annealing at Extreme Temperatures. *Adv. Mater.* **2016**, *28*, 6598–6605.

(13) Gu, X.; Fan, Q.; Yang, F.; Cai, L.; Zhang, N.; Zhou, W.; Zhou, W.; Xie, S. Hydro-Actuation of Hybrid Carbon Nanotube Yarn Muscles. *Nanoscale* **2016**, *8*, 17881–17886.

(14) Kim, S. H.; Kwon, C. H.; Park, K.; Mun, T. J.; Lepró, X.; Baughman, R. H.; Spinks, G. M.; Kim, S. J. Bio-Inspired, Moisture-Powered Hybrid Carbon Nanotube Yarn Muscles. *Sci. Rep.* **2016**, *6*, 23016.

(15) Jin, K.; Zhang, S.; Zhou, S.; Qiao, J.; Song, Y.; Di, J.; Zhang, D.; Li, Q. Self-Plied and Twist-Stable Carbon Nanotube Yarn Artificial Muscles Driven by Organic Solvent Adsorption. *Nanoscale* **2018**, *10*, 8180–8186.

(16) Mu, J.; de Andrade, M. J.; Fang, S.; Wang, X.; Gao, E.; Li, N.; Kim, S. H.; Wang, H.; Hou, C.; Zhang, Q.; Zhu, M.; Qian, D.; Lu, H.; Kongahage, D.; Talebian, S.; Foroughi, J.; Spinks, G.; Kim, H.; Ware, T. H.; Sim, H. J.; Lee, D. Y.; Jang, Y.; Kim, S. J.; Baughman, R. H. Sheath-Run Artificial Muscles. *Science* **2019**, *365*, 150–155.

(17) Wang, Y.; Qiao, J.; Wu, K.; Yang, W.; Ren, M.; Dong, L.; Zhou, Y.; Wu, Y.; Wang, X.; Yong, Z.; Di, J.; Li, Q. High-Twist-Pervaded Electrochemical Yarn Muscles with Ultralarge and Fast Contractile Actuations. *Materials Horizons* **2020**, *7*, 3043–3050.

(18) Chu, H.; Hu, X.; Wang, Z.; Mu, J.; Li, N.; Zhou, X.; Fang, S.; Haines, C. S.; Park, J. W.; Qin, S.; Yuan, N.; Xu, J.; Tawfick, S.; Kim, H.; Conlin, P.; Cho, M.; Cho, K.; Oh, J.; Nielsen, S.; Alberto, K. A.; Razal, J. M.; Foroughi, J.; Spinks, G. M.; Kim, S. J.; Ding, J.; Leng, J.; Baughman, R. H. Unipolar Stroke, Electroosmotic Pump Carbon Nanotube Yarn Muscles. *Science* **2021**, *371*, 494–498.

(19) Ren, M.; Qiao, J.; Wang, Y.; Wu, K.; Dong, L.; Shen, X.; Zhang, H.; Yang, W.; Wu, Y.; Yong, Z.; Chen, W.; Zhang, Y.; Di, J.; Li, Q. Strong and Robust Electrochemical Artificial Muscles by Ionic-Liquid-in-Nanofiber-Sheathed Carbon Nanotube Yarns. *Small* **2021**, *17*, 2006181.

(20) Choi, C.; Kim, S. H.; Sim, H. J.; Lee, J. A.; Choi, A. Y.; Kim, Y. T.; Lepró, X.; Spinks, G. M.; Baughman, R. H.; Kim, S. J. Stretchable, Weavable Coiled Carbon Nanotube/MnO₂/Polymer Fiber Solid-State Supercapacitors. *Sci. Rep.* **2015**, *5*, 9387.

- (21) Yu, J.; Lu, W.; Smith, J. P.; Booksh, K. S.; Meng, L.; Huang, Y.; Li, Q.; Byun, J.-H.; Oh, Y.; Yan, Y.; Chou, T.-W. A High Performance Stretchable Asymmetric Fiber-Shaped Supercapacitor with a Core-Sheath Helical Structure. *Adv. Energy Mater.* **2017**, *7*, 1600976.
- (22) Choi, C.; Sim, H. J.; Spinks, G. M.; Lepró, X.; Baughman, R. H.; Kim, S. J. Elastomeric and Dynamic MnO₂/CNT Core–Shell Structure Coiled Yarn Supercapacitor. *Adv. Energy Mater.* **2016**, *6*, 1502119.
- (23) Choi, C.; Kim, J. H.; Sim, H. J.; Di, J.; Baughman, R. H.; Kim, S. J. Microscopically Buckled and Macroscopically Coiled Fibers for Ultra-Stretchable Supercapacitors. *Adv. Energy Mater.* **2017**, *7*, 1602021.
- (24) Choi, C.; Kim, K. M.; Kim, K. J.; Lepró, X.; Spinks, G. M.; Baughman, R. H.; Kim, S. J. Improvement of System Capacitance via Weavable Superelastic Biscrolled Yarn Supercapacitors. *Nat. Commun.* **2016**, *7*, 13811.
- (25) Son, W.; Chun, S.; Lee, J. M.; Lee, Y.; Park, J.; Suh, D.; Lee, D. W.; Jung, H.; Kim, Y.-J.; Kim, Y.; Jeong, S. M.; Lim, S. K.; Choi, C. Highly Twisted Supercoils for Superelastic Multifunctional Fibres. *Nat. Commun.* **2019**, *10*, 426.
- (26) Zhang, Y.; Bai, W.; Cheng, X.; Ren, J.; Weng, W.; Chen, P.; Fang, X.; Zhang, Z.; Peng, H. Flexible and Stretchable Lithium-Ion Batteries and Supercapacitors Based on Electrically Conducting Carbon Nanotube Fiber Springs. *Angew. Chem., Int. Ed.* **2014**, *53*, 14564–14568.
- (27) Lee, J. M.; Chun, S.; Son, W.; Suh, D.; Kim, S. H.; Kim, H.; Lee, D.; Kim, Y.; Kim, Y.-K.; Lim, S. K.; Choi, C. DNA-Inspired, Highly Packed Supercoil Battery for Ultra-High Stretchability and Capacity. *Nano Energy* **2021**, *85*, 106034.
- (28) Volodin, A.; Buntinx, D.; Ahlskog, M.; Fonseca, A.; Nagy, J. B.; Van Haesendonck, C. Coiled Carbon Nanotubes as Self-Sensing Mechanical Resonators. *Nano Lett.* **2004**, *4*, 1775–1779.
- (29) Li, Y.; Shang, Y.; He, X.; Peng, Q.; Du, S.; Shi, E.; Wu, S.; Li, Z.; Li, P.; Cao, A. Overtwisted, Resolvable Carbon Nanotube Yarn Entanglement as Strain Sensors and Rotational Actuators. *ACS Nano* **2013**, *7*, 8128–8135.
- (30) Shang, Y.; Li, Y.; He, X.; Zhang, L.; Li, Z.; Li, P.; Shi, E.; Wu, S.; Cao, A. Elastic Carbon Nanotube Straight Yarns Embedded with Helical Loops. *Nanoscale* **2013**, *5*, 2403–2410.
- (31) Shang, Y.; Hua, C.; Xu, W.; Hu, X.; Wang, Y.; Zhou, Y.; Zhang, Y.; Li, X.; Cao, A. Meter-Long Spiral Carbon Nanotube Fibers Show Ultrauniformity and Flexibility. *Nano Lett.* **2016**, *16*, 1768–1775.
- (32) Jang, Y.; Kim, S. M.; Kim, K. J.; Sim, H. J.; Kim, B.-J.; Park, J. W.; Baughman, R. H.; Ruhparwar, A.; Kim, S. J. Self-Powered Coiled Carbon-Nanotube Yarn Sensor for Gastric Electronics. *ACS Sensors* **2019**, *4*, 2893–2899.
- (33) Gao, Y.; Guo, F.; Cao, P.; Liu, J.; Li, D.; Wu, J.; Wang, N.; Su, Y.; Zhao, Y. Winding-Locked Carbon Nanotubes/Polymer Nanofibers Helical Yarn for Ultrastretchable Conductor and Strain Sensor. *ACS Nano* **2020**, *14*, 3442–3450.
- (34) Tran, C. D.; Humphries, W.; Smith, S. M.; Huynh, C.; Lucas, S. Improving the Tensile Strength of Carbon Nanotube Spun Yarns Using a Modified Spinning Process. *Carbon* **2009**, *47*, 2662–2670.
- (35) Hou, G.; Wang, G.; Deng, Y.; Zhang, J.; Nshimiyimana, J. P.; Chi, X.; Hu, X.; Chu, W.; Dong, H.; Zhang, Z.; Liu, L.; Sun, L. Effective Enhancement of the Mechanical Properties of Macroscopic Single-Walled Carbon Nanotube Fibers by Pressure Treatment. *RSC Adv.* **2016**, *6*, 97012–97017.
- (36) Hill, F. A.; Havel, T. F.; Hart, A. J.; Livermore, C. Enhancing the Tensile Properties of Continuous Millimeter-Scale Carbon Nanotube Fibers by Densification. *ACS Appl. Mater. Interfaces* **2013**, *5*, 7198–7207.
- (37) Lin, S.; Wang, Z.; Chen, X.; Ren, J.; Ling, S. Ultrastrong and Highly Sensitive Fiber Microactuators Constructed by Force-Reeled Silks. *Advanced Science* **2020**, *7*, 1902743.
- (38) Marega, R.; Accorsi, G.; Meneghetti, M.; Parisini, A.; Prato, M.; Bonifazi, D. Cap Removal and Shortening of Double-Walled and Very-Thin Multi-Walled Carbon Nanotubes under Mild Oxidative Conditions. *Carbon* **2009**, *47*, 675–682.
- (39) Meng, F.; Zhao, J.; Ye, Y.; Zhang, X.; Li, Q. Carbon Nanotube Fibers for Electrochemical Applications: Effect of Enhanced Interfaces by An Acid Treatment. *Nanoscale* **2012**, *4*, 7464–7468.
- (40) Xu, Z.; Sun, H.; Zhao, X.; Gao, C. Ultrastrong Fibers Assembled from Giant Graphene Oxide Sheets. *Adv. Mater.* **2013**, *25*, 188–193.
- (41) Li, W.; Xu, F.; Wang, Z.; Wu, J.; Liu, W.; Qiu, Y. Effect of Thermal Treatments on Structures and Mechanical Properties of Aerogel-Spun Carbon Nanotube Fibers. *Mater. Lett.* **2016**, *183*, 117–121.
- (42) Peng, Q.; Li, Y.; He, X.; Gui, X.; Shang, Y.; Wang, C.; Wang, C.; Zhao, W.; Du, S.; Shi, E.; Li, P.; Wu, D.; Cao, A. Graphene Nanoribbon Aerogels Unzipped from Carbon Nanotube Sponges. *Adv. Mater.* **2014**, *26*, 3241–3247.
- (43) Beese, A. M.; Sarkar, S.; Nair, A.; Naraghi, M.; An, Z.; Moravsky, A.; Loutfy, R. O.; Buehler, M. J.; Nguyen, S. T.; Espinosa, H. D. Bio-Inspired Carbon Nanotube-Polymer Composite Yarns with Hydrogen Bond-Mediated Lateral Interactions. *ACS Nano* **2013**, *7*, 3434–3446.
- (44) Ziegler, K. J.; Gu, Z.; Peng, H.; Flor, E. L.; Hauge, R. H.; Smalley, R. E. Controlled Oxidative Cutting of Single-Walled Carbon Nanotubes. *J. Am. Chem. Soc.* **2005**, *127*, 1541–1547.
- (45) Lee, W. H.; Kim, S. J.; Lee, W. J.; Lee, J. G.; Haddon, R. C.; Reucroft, P. J. X-ray Photoelectron Spectroscopic Studies of Surface Modified Single-Walled Carbon Nanotube Material. *Appl. Surf. Sci.* **2001**, *181*, 121–127.
- (46) He, S.; Zhang, Y.; Qiu, L.; Zhang, L.; Xie, Y.; Pan, J.; Chen, P.; Wang, B.; Xu, X.; Hu, Y.; Dinh, C. T.; De Luna, P.; Banis, M. N.; Wang, Z.; Sham, T.-K.; Gong, X.; Zhang, B.; Peng, H.; Sargent, E. H. Chemical-to-Electricity Carbon: Water Device. *Adv. Mater.* **2018**, *30*, 1707635.
- (47) He, S.; Chen, P.; Qiu, L.; Wang, B.; Sun, X.; Xu, Y.; Peng, H. A Mechanically Actuating Carbon-Nanotube Fiber in Response to Water and Moisture. *Angew. Chem.* **2015**, *127*, 15093–15097.
- (48) He, S.; Hu, Y.; Wan, J.; Gao, Q.; Wang, Y.; Xie, S.; Qiu, L.; Wang, C.; Zheng, G.; Wang, B.; Peng, H. Biocompatible Carbon Nanotube Fibers for Implantable Supercapacitors. *Carbon* **2017**, *122*, 162–167.
- (49) Adusei, P. K.; Gbordzoe, S.; Kanakaraj, S. N.; Hsieh, Y.-Y.; Alvarez, N. T.; Fang, Y.; Johnson, K.; McConnell, C.; Shanov, V. Fabrication and Study of Supercapacitor Electrodes Based on Oxygen Plasma Functionalized Carbon Nanotube Fibers. *Journal of Energy Chemistry* **2020**, *40*, 120–131.
- (50) Yu, H.; Cheng, D.; Williams, T. S.; Severino, J.; De Rosa, I. M.; Carlson, L.; Hicks, R. F. Rapid Oxidative Activation of Carbon Nanotube Yarn and Sheet by a Radio Frequency, Atmospheric Pressure, Helium and Oxygen Plasma. *Carbon* **2013**, *57*, 11–21.
- (51) Shao, Y.; Xu, F.; Marriam, I.; Liu, W.; Gao, Z.; Qiu, Y. Quasi-Static and Dynamic Interfacial Evaluations of Plasma Functionalized Carbon Nanotube Fiber. *Appl. Surf. Sci.* **2019**, *465*, 795–801.
- (52) Park, O.-K.; Young Kim, W.; Min Kim, S.; You, N.-H.; Jeong, Y.; Su Lee, H.; Ku, B.-C. Effect of Oxygen Plasma Treatment on the Mechanical Properties of Carbon Nanotube Fibers. *Mater. Lett.* **2015**, *156*, 17–20.
- (53) Choi, C.; Lee, J. A.; Choi, A. Y.; Kim, Y. T.; Lepró, X.; Lima, M. D.; Baughman, R. H.; Kim, S. J. Flexible Supercapacitor Made of Carbon Nanotube Yarn with Internal Pores. *Adv. Mater.* **2014**, *26*, 2059–2065.
- (54) Yu, D.; Goh, K.; Zhang, Q.; Wei, L.; Wang, H.; Jiang, W.; Chen, Y. Controlled Functionalization of Carbonaceous Fibers for Asymmetric Solid-State Micro-Supercapacitors with High Volumetric Energy Density. *Adv. Mater.* **2014**, *26*, 6790–6797.
- (55) Cheng, X.; Zhang, J.; Ren, J.; Liu, N.; Chen, P.; Zhang, Y.; Deng, J.; Wang, Y.; Peng, H. Design of a Hierarchical Ternary Hybrid for a Fiber-Shaped Asymmetric Supercapacitor with High Volumetric Energy Density. *J. Phys. Chem. C* **2016**, *120*, 9685–9691.
- (56) Lee, J. A.; Shin, M. K.; Kim, S. H.; Cho, H. U.; Spinks, G. M.; Wallace, G. G.; Lima, M. D.; Lepró, X.; Kozlov, M. E.; Baughman, R. H.; Kim, S. J. Ultrafast Charge and Discharge Biscrolled Yarn

Supercapacitors for Textiles and Microdevices. *Nat. Commun.* **2013**, *4*, 1970.

(57) Wang, K.; Meng, Q.; Zhang, Y.; Wei, Z.; Miao, M. High-Performance Two-Ply Yarn Supercapacitors Based on Carbon Nanotubes and Polyaniline Nanowire Arrays. *Adv. Mater.* **2013**, *25*, 1494–1498.

(58) Elettro, H.; Neukirch, S.; Vollrath, F.; Antkowiak, A. In-Drop Capillary Spooling of Spider Capture Thread Inspires Hybrid Fibers with Mixed Solid–Liquid Mechanical Properties. *Proc. Natl. Acad. Sci. U. S. A.* **2016**, *113*, 6143–6147.

(59) Lee, J. A.; Li, N.; Haines, C. S.; Kim, K. J.; Lepró, X.; Ovalle-Robles, R.; Kim, S. J.; Baughman, R. H. Electrochemically Powered, Energy-Conserving Carbon Nanotube Artificial Muscles. *Adv. Mater.* **2017**, *29*, 1700870.

(60) Foroughi, J.; Spinks, G. M.; Wallace, G. G.; Oh, J.; Kozlov, M. E.; Fang, S.; Mirfakhrai, T.; Madden, J. D. W.; Shin, M. K.; Kim, S. J.; Baughman, R. H. Torsional Carbon Nanotube Artificial Muscles. *Science* **2011**, *334*, 494–497.

(61) Mirfakhrai, T.; Oh, J.; Kozlov, M.; Fok, E. C. W.; Zhang, M.; Fang, S.; Baughman, R. H.; Madden, J. D. W. Electrochemical Actuation of Carbon Nanotube Yarns. *Smart Mater. Struct.* **2007**, *16*, 243–249.

(62) Yamada, T.; Hayamizu, Y.; Yamamoto, Y.; Yomogida, Y.; Izadi-Najafabadi, A.; Futaba, D. N.; Hata, K. A Stretchable Carbon Nanotube Strain Sensor for Human-Motion Detection. *Nat. Nanotechnol.* **2011**, *6*, 296–301.

(63) Wu, G.; Tan, P.; Wu, X.; Peng, L.; Cheng, H.; Wang, C.-F.; Chen, W.; Yu, Z.; Chen, S. High-Performance Wearable Micro-Supercapacitors based on Microfluidic-Directed Nitrogen-Doped Graphene Fiber Electrodes. *Adv. Funct. Mater.* **2017**, *27*, 1702493.

(64) Lota, G.; Tyczkowski, J.; Kapica, R.; Lota, K.; Frackowiak, E. Carbon Materials Modified by Plasma Treatment as Electrodes for Supercapacitors. *J. Power Sources* **2010**, *195*, 7535–7539.

(65) Banks, C. E.; Davies, T. J.; Wildgoose, G. G.; Compton, R. G. Electrocatalysis at Graphite and Carbon Nanotube Modified Electrodes: Edge-Plane Sites and Tube Ends are The Reactive Sites. *Chem. Commun.* **2005**, *7*, 829–841.

(66) Xiao, X.; Li, T.; Peng, Z.; Jin, H.; Zhong, Q.; Hu, Q.; Yao, B.; Luo, Q.; Zhang, C.; Gong, L.; Chen, J.; Gogotsi, Y.; Zhou, J. Freestanding Functionalized Carbon Nanotube-based Electrode for Solid-State Asymmetric Supercapacitors. *Nano Energy* **2014**, *6*, 1–9.

(67) Frackowiak, E.; Béguin, F. Carbon Materials for the Electrochemical Storage of Energy in Capacitors. *Carbon* **2001**, *39*, 937–950.

(68) Rihm, J.; Sim, E. S.; Cho, S. B.; Chung, Y.-C. Enhancement of the Quantum Capacitances of Group-14 Elemental Twodimensional Materials by Ti-Doping: A First Principles Study. *Appl. Surf. Sci.* **2020**, *530*, 147301.

(69) Kim, S. H.; Haines, C. S.; Li, N.; Kim, K. J.; Mun, T. J.; Choi, C.; Di, J.; Oh, Y. J.; Oviedo, J. P.; Bykova, J.; Fang, S.; Jiang, N.; Liu, Z.; Wang, R.; Kumar, P.; Qiao, R.; Priya, S.; Cho, K.; Kim, M.; Lucas, M. S.; Drummy, L. F.; Maruyama, B.; Lee, D. Y.; Lepró, X.; Gao, E.; Albarq, D.; Ovalle-Robles, R.; Kim, S. J.; Baughman, R. H. Harvesting Electrical Energy from Carbon Nanotube Yarn Twist. *Science* **2017**, *357*, 773–778.

(70) Kresse, G.; Furthmüller, J. Efficient Iterative Schemes for Ab Initio Total-Energy Calculations Using a Plane-Wave Basis Set. *Phys. Rev. B* **1996**, *54*, 11169–11186.

(71) Blöchl, P. E. Projector Augmented-Wave Method. *Phys. Rev. B* **1994**, *50*, 17953–17979.

(72) Perdew, J. P.; Burke, K.; Ernzerhof, M. Generalized Gradient Approximation Made Simple. *Phys. Rev. Lett.* **1996**, *77*, 3865–3868.

(73) Henkelman, G.; Arnaldsson, A.; Jónsson, H. A Fast and Robust Algorithm for Bader Decomposition of Charge Density. *Comput. Mater. Sci.* **2006**, *36*, 354–360.



CAS BIOFINDER DISCOVERY PLATFORM™

BRIDGE BIOLOGY AND CHEMISTRY FOR FASTER ANSWERS

Analyze target relationships,
compound effects, and disease
pathways

Explore the platform

